CrossMark

ORIGINAL ARTICLE

Collateralization of projections from the paraventricular nucleus of the thalamus to the nucleus accumbens, bed nucleus of the stria terminalis, and central nucleus of the amygdala

Xinwen Dong[1] · Sa Li[1] · Gilbert J. Kirouac[1,2]

Abstract The paraventricular nucleus of the thalamus (PVT) is a midline thalamic nucleus with dense projections to the nucleus accumbens (NAc), dorsolateral region of the bed nucleus of the stria terminalis (BSTDL) and the lateral/capsular region of the central nucleus of the amygdala (CeL/CeC). Recent experimental evidence indicates that the PVT is involved in both appetitive and aversive behaviors. However, it is unknown if subgroups of neurons in the PVT innervate different subcortical targets or if the same neurons issue collaterals to multiple areas. To address this issue, we injected two different fluorescent retrograde tracers, cholera toxin subunit B conjugated to Alexa Fluor-488 or Alexa Fluor-594, into different pairs of the subcortical targets including different parts of the NAc (shell, core, dorsomedial shell, and ventromedial shell), BSTDL, and amygdala (basolateral amygdala and CeL/CeC). The results indicate a moderate to high level of collateralization of projections from neurons in the PVT to NAc, BSTDL, and CeL/CeC suggesting a potential importance of the PVT in simultaneously coordinating the activity of key regions of the brain involved in mediating emotional and motivational behaviors. We also observed a difference in the subcortical targets innervated by the anterior PVT (aPVT) and posterior PVT (pPVT) showing that more neurons in the aPVT innervate the dorsomedial part of the NAc shell, while more neurons in the pPVT innervate the ventromedial NAc shell, BSTDL, and CeL/CeC. This observation is suggestive of a potential functional difference between the aPVT and pPVT.

Abbreviations

3V	Third ventricle
ac	Anterior commissure
aca	Anterior commissure, anterior limb
AF	Alexa Fluor
AM	Anteromedial nucleus of thalamus
BLA	Basolateral amygdala
BLP	Basolateral amygdala, posterior
BST	Bed nucleus of stria terminalis
BSTDL	Bed nucleus of stria terminalis, dorsolateral
BSTM	Bed nucleus of stria terminalis, medial
CeA	Central nucleus of the amygdala
CeC	Central amygdala, capsular
CeL	Central amygdala, lateral
CeM	Central amygdala, medial
CM	Central medial nucleus of thalamus
CPu	Caudate putamen
CTb	Cholera toxin subunit B
DB	Double labeled
Hb	Habenular nucleus
IAM	Interanteromedial nucleus of thalamus
ic	Internal capsule
IMD	Intermediodorsal nucleus of thalamus
MD	Mediodorsal nucleus of thalamus
NAc	Nucleus accumbens

✉ Gilbert J. Kirouac
Gilbert.Kirouac@umanitoba.ca

1 Department of Oral Biology, College of Dentistry, Rady Faculty of Health Sciences, University of Manitoba, 780 Bannatyne Avenue, Winnipeg, MB R3E 0W2, Canada

2 Department of Psychiatry, College of Medicine, Rady Faculty of Health Sciences, University of Manitoba, Winnipeg, MB R3E 0W2, Canada

🍛 Springer

NAcC	Nucleus accumbens core
NAcSh, dm, vm	Nucleus accumbens shell, dorsomedial and ventromedial parts
opt	Optic tract
PC	Paracentral nucleus of thalamus
PT	Paratenial nucleus of thalamus
PVT, a, p	Paraventricular nucleus of thalamus, anterior and posterior parts
Re	Nucleus reuniens of thalamus

Introduction

The paraventricular nucleus of the thalamus (PVT) is a member of the group of midline and intralaminar thalamic nuclei that have been traditionally associated with functions related to general arousal, attention, and consciousness (Bentivoglio et al. 1991; Groenewegen and Berendse 1994). Anatomical studies have shown that members of the midline and intralaminar nuclei project to different regions of the cerebral cortex and striatum indicating that different members of this group of thalamic nuclei can influence brain mechanisms associated with functionally specialized cortical–subcortical circuits (Groenewegen and Berendse 1994; Smith et al. 2004; Van der Werf et al. 2002). The fact that the PVT innervates the prefrontal cortex and the nucleus accumbens (NAc) of the ventral striatum has been taken as anatomical evidence that the PVT could influence motivational and emotional behavior (Hsu and Price 2009; Li and Kirouac 2008; Moga et al. 1995; Vertes and Hoover 2008). Recent experimental evidence shows that manipulations that affect the activity of neurons in the PVT or its fiber projections can influence a broad range of behaviors including those involved in food reward (Choi et al. 2010; Labouebe et al. 2016), drug seeking (Barson et al. 2015, 2017; Browning et al. 2014; Hamlin et al. 2009; James et al. 2010; Matzeu et al. 2015, 2016; Neumann et al. 2016; Young and Deutch 1998), learned fear (Do-Monte et al. 2015; Li et al. 2014; Padilla-Coreano et al. 2012; Penzo et al. 2015), conditioned place avoidance (Li et al. 2011; Zhu et al. 2016) and anxiety-like behaviors (Barson and Leibowitz 2015; Dong et al. 2015; Heydendael et al. 2011; Li et al. 2009, 2010a, b). These studies, in addition to studies using c-fos expression to anatomically map neuronal activation, indicate that the PVT regulates behaviors with both negative and positive emotional valences (Hsu et al. 2014; Kirouac 2015).

Anterograde tracing studies have provided a comprehensive picture of the areas of the brain most densely innervated by the PVT (Li and Kirouac 2008; Moga et al. 1995; Vertes and Hoover 2008). These studies reported very dense labeling of fibers in the NAc, bed nucleus of the stria terminalis (BST) and the central nucleus of the

amygdala (CeA). This is in contrast to the infralimbic, prelimbic, and insular cortex as well as other subcortical areas that had relatively weaker fiber labeling (Li and Kirouac 2008). This suggests that the PVT may exert a profound influence on brain function through projections to the NAc, BST, and CeA (Kirouac 2015; Li and Kirouac 2008). Indeed, recent studies have provided evidence that projections from the PVT to the NAc and CeA modulate some aspect of behavior. For instance, optogenetic activation of the projection from the PVT to the NAc was reported to increase sucrose-seeking (Labouebe et al. 2016) and disruption of synaptic transmission between the PVT and the NAc was found to decrease cocaine self-administration (Neumann et al. 2016). Another recent study reported that optogenetic and chemogenetic inhibition of the PVT fibers in the NAc attenuated the acquisition of conditioned place avoidance to morphine withdrawal, footshocks, and lithium chloride in mice (Zhu et al. 2016). The behavioral effects produced by experimental manipulation of PVT afferents to the NAc are consistent with the well-known influence of the NAc in appetitive and defensive behaviors (Berridge and Kringelbach 2015; Floresco 2015; Nicola 2007; Pennartz et al. 1994). Optogenetic and chemogenetic silencing of a projection from the PVT to the CeA was also reported to attenuate behavioral freezing to an auditory cue previously associated with footshocks (Do-Monte et al. 2015; Penzo et al. 2015), which is in line with the well-known contribution of the CeA in learned fear (Ehrlich et al. 2009; Pape and Pare 2010). Consequently, a number of studies indicate that the PVT can modulate different types of behaviors in a projection-specific manner.

The most obvious explanation of how the PVT can influence behaviors with different emotional valences is that subpopulations of neurons in the PVT exert their effects in a projection-specific manner. For example, PVT neurons that influence a defensive behavior like fear may target subcortical regions that specifically modulate freezing, whereas PVT neurons that influence drug seeking may target subcortical regions that control approach. However, the question of whether the PVT consists of subpopulations of neurons with unique projections has not been addressed adequately. This is especially important to consider since single neurons in the brain often have axons that bifurcate to produce fiber collaterals that innervate multiple regions of the brain (Parent et al. 2000; Prensa et al. 2009) and this is particularly true of neurons projecting to deep telencephalic nuclei (Reichard et al. 2016). A number of papers have addressed the extent of collateralization of PVT neurons to the cortex or cortical-like structure and subcortical areas by injecting two different retrograde tracers in selective targets of the PVT. Most of these studies indicate that despite being largely intermingled, neurons

that project to the NAc and CeA are mostly separate from those that project to the prefrontal cortex, ventral subiculum of the hippocampus and the basolateral amygdala (Bubser and Deutch 1998; Penzo et al. 2015; Su and Bentivoglio 1990). This is in contrast to one study that found a large number of neurons in the PVT projected to both the prefrontal cortex and the NAc (Otake and Nakamura 1998). Furthermore, single neuron tracing of a small number of cells in the PVT showed that a neuron in the PVT innervated multiple subcortical nuclei before issuing a fiber to the cortex (Unzai et al. 2017). While it is likely that some neurons issue collaterals to different regions of the forebrain, the extent of this collateralization has not been addressed adequately.

The present study focuses on the question of whether, or to what extent, neurons in the PVT that project to its main subcortical targets originate from distinct subpopulations and to determine the relative location of these subpopulations along the anterior–posterior aspect of the PVT. To address this issue, we injected two different fluorescent retrograde tracers into different pairs of subcortical targets most densely innervated by the PVT. The areas selected were based on a comprehensive study of the PVT projections showing that the shell (NAcSh) and core (NAcC) portions of the NAc; the lateral (CeL) and capsular (CeC) parts of the CeA; and the dorsolateral part of BST (BSTDL) are the most densely innervated regions of the forebrain (Li and Kirouac 2008). Detailed maps of the location and counts of labeled neurons in the PVT were carried out to determine the extent of segregation and collateralization of these PVT projections.

Methods

Animals

A total of 61 male Sprague–Dawley rats (University of Manitoba vivarium) weighing 300 ± 10 g received injections of the tracers, of which 24 rats were used to generate the figures and data presented in this study. Animals were housed on a 12:12 h light–dark cycle with food and water freely available. The experimental procedures were in compliance with the Canadian Council on Animal Care and the experimental protocol was approved by Research Ethics Review Board of the University of Manitoba.

Retrograde tracing

Animals were anesthetized with 2–3% isoflurane and given meloxicam (2 mg/kg, s.c.) for post-surgery pain management. Animals were placed in a Stoelting stereotaxic frame and a hand drill was used to expose the brain surface above the target sites. Pressure injections of retrograde tracers were done using glass pipettes with outer diameter of approximately 37–40 μm. Injections of tracers were done in the following areas using coordinates derived from a stereotaxic atlas of the rat brain (Paxinos and Watson 2009): NAcSh, 1.5 mm anterior, 0.9–1.1 mm lateral, 6.0–7.5 mm ventral; NAcC, 1.5 mm anterior, 1.8 mm lateral, 6.5 mm ventral; BSTDL, 0.3 mm anterior, 1.6 mm lateral, 6.0 mm ventral; CeL/CeC, 2.1 mm posterior, 4.2 mm lateral, 7.5 mm ventral; basolateral amygdala (BLA), 2.5 mm posterior, 4.9 mm lateral, 7.8 mm ventral (all coordinates are relative to bregma and the dural surface of the brain). The retrograde tracer cholera toxin subunit B conjugated to Alexa Fluor-488 (AF-CTb-488; catalogue No. C22841, Invitrogen, Calsbad, CA, USA) and Alexa Fluor-594 (AF-CTb-594; catalogue No. C22842, Invitrogen) were dissolved in 0.06 M neutral phosphate buffer (PB) at 0.5% concentration and 50 nl of the tracer was injected over 10–15 min using a picospritzer into one of the two regions of interest in the same hemisphere of the brain. Four cases of each combination were used for analysis: NAcSh and CeL/CeC; NAcSh and BSTDL; BSTDL and CeL/CeC; CeL/CeC and BLA; NAcSh and NAcC; dorsomedial NAcSh (dmNAcSh) and ventromedial NAcSh (vmNAcSh). The pipette was kept in situ for another 10 min before removal to prevent leakage. The scalp incisions were sutured and rats were returned to their home cages for recovery.

Histology

After a 7- to 9-day postoperative survival, animals were deeply anesthetized with 10% chloral hydrate (600 mg/kg, i.p.) and transcardially perfused with 150 ml heparinized saline followed by 400–500 ml ice-cold 4% paraformaldehyde in 0.1 M PB (pH 7.4). The brains were removed and post-fixed in the same fixative for 4–5 h, and cryoprotected in 20% sucrose with 10% glycerin over 2 days at 4 °C. Coronal sections of the brain containing the injection sites and the PVT were taken at 50 μm and sections were mounted on slide at every 200 μm for subsequent examination under a fluorescent microscope. The sections were dehydrated through a series of graded alcohol solutions, cleared with CitriSolv (Fisher Scientific, ON, Canada), and coverslipped with mounting medium.

Alternate brain sections containing the injected areas and the PVT region were selected for the NeuN staining. The immunohistochemical reactions were carried out at room temperature on free-floating sections. Primary and secondary antibodies were diluted in blocking solution containing 0.1% sodium azide, 0.3% Triton X-100, and 5% normal donkey serum in 0.1 M PBS. Brain sections were pre-incubated in the blocking solution for 1 h and then

incubated in primary mouse anti-NeuN antibody (1:1000; catalogue No. MAB377, Chemicon, Temecula, CA, USA) overnight. After 3 rinses in PBS, sections were transferred into a biotinylated donkey anti-mouse (1:500; Jackson Immunoresearch, West Grove, PA, USA) antiserum for 1 h. Then sections were rinsed thoroughly and incubated with an avidin–biotin complex (ABC) solution (Elite ABC kit; Vector Laboratories, Burlingame, CA, USA) for 1 h. After three more rinsing steps, sections were reacted with diaminobenzidine tetrachloride (DAB) with nickel intensification (Vector DAB Kit) to produce a black reaction product. The DAB reaction was terminated by rinsing the sections with PBS and the sections were mounted on slides, air dried and coverslipped with mounting medium.

Data analysis

Brain sections were examined and photographed using an Olympus BX51 microscope equipped with a digital camera (SPOT RT Slicer, Diagnostic Instruments Inc, Sterling Heights, MI, USA). Injection sites were drawn based on photos taken under $40\times$ magnification and the distribution of fluorescent labeled cells in the PVT were drawn based on merged sets of images taken at $200\times$ magnification. The stereotaxic levels chosen for these illustrations were those that are representative of the distribution of labeled cells in the PVT and adjacent thalamic nuclei. The NeuN-stained sections were used in combination with a stereotaxic atlas to identify and draw the anatomical demarcations of brain regions (Paxinos and Watson 2009). Calibration bars were inserted using SPOT software (Version 3.2, Diagnostic Instruments) and the images were transferred to Adobe Photoshop CS4 to optimize light and contrast levels.

The total numbers of NeuN and fluorescent labeled cells in the PVT were counted on sections 200 μm apart starting at the level of the aPVT (1.08 mm posterior to bregma) to the pPVT (3.96 mm posterior to bregma) according to a standard atlas of the rat brain (Paxinos and Watson 2009). The presence of fluorescent labeled neurons in the PVT was examined under appropriate filters and counts of single-labeled neurons were made under $200\times$ magnification. Double-labeled neurons were identified under $200\times$ magnification and always verified under $400\times$ magnification and by focusing through the labeled neurons. The data represent the mean of the cell counts done independently by two experimenters. The count data for all the sections analyzed were subdivided into aPVT and pPVT levels (eight sections each) with stereotaxic level 2.5 mm posterior to bregma as the divide. Likewise, the number of NeuN-stained neurons in the PVT was counted in four cases on the sections corresponding to the approximate stereotaxic levels used for counting the number of fluorescent labeled neurons. The total number of NeuN-stained neurons for these sections was divided in half since the retrogradely labeled neurons were found only on the ipsilateral side of the injection sites. The mean of the NeuN labeled cells was used to estimate the proportion of CTb-labeled cells in the PVT in all the cases (CTb-labeled cells/NeuN-labeled cells $\times$ 100%). A two-way ANOVA was used to analyze the proportion of labeled cells with levels (aPVT vs pPVT) and tracer target sites as independent variables. Bonferroni post hoc test was used for further comparison.

Results

Injections

Four cases for each pair were selected based on the criteria that the injections were restricted to targeted regions and were approximately of similar size in terms of the diffusion of the tracer. The cases discarded were those with an injection that was off target or that had injections that were visibly smaller than the typical injection site selected for the study. Figure 1 shows one representative case with injection sites in the NAcSh and CeL/CeC as well as the retrograde labeling in the aPVT and pPVT resulted from these injections. The dense cores of the tracers were largely confined to the medial shell of NAc and the lateral portion of CeA (CeL/CeC). The pattern of fluorescent labeling observed was consistent to that observed in a previous study using immunohistochemical staining with DAB (Li and Kirouac 2008). Regions around the dense cores also contained more diffuse AF-CTb. However, it is unlikely that fibers to areas of diffuse AF-CTb produce observable retrograde transport in the PVT (Luppi et al. 1990). The pairs of injection sites selected for analysis are schematically illustrated in Fig. 2. For the combinations of NAcSh and CeL/CeC, NAcSh and BSTDL, NAcSh and NAcC, the injections to the NAcSh were confined to the medial region of the shell.

The conjugate of CTb used was reversed in some of the injections to evaluate the uptake and transport of the different conjugates (see Fig. 2 for placement of different conjugates in the same regions). For example, the number of labeled neurons in the PVT in cases with AF-CTb-594 injections in the BSTDL (2217 ± 385, $n = 4$) was very close to the same as the number counted when AF-CTb-488 was injected to the BSTDL (2221 ± 331, $n = 4$). Similarly, the number of labeled neurons in the PVT in cases with AF-CTb-594 injections in the CeL/CeC (1354 ± 176; $n = 7$) was comparable to the number when AF-CTb-488 was injected to the CeL/CeC (1272 ± 233; $n = 3$).
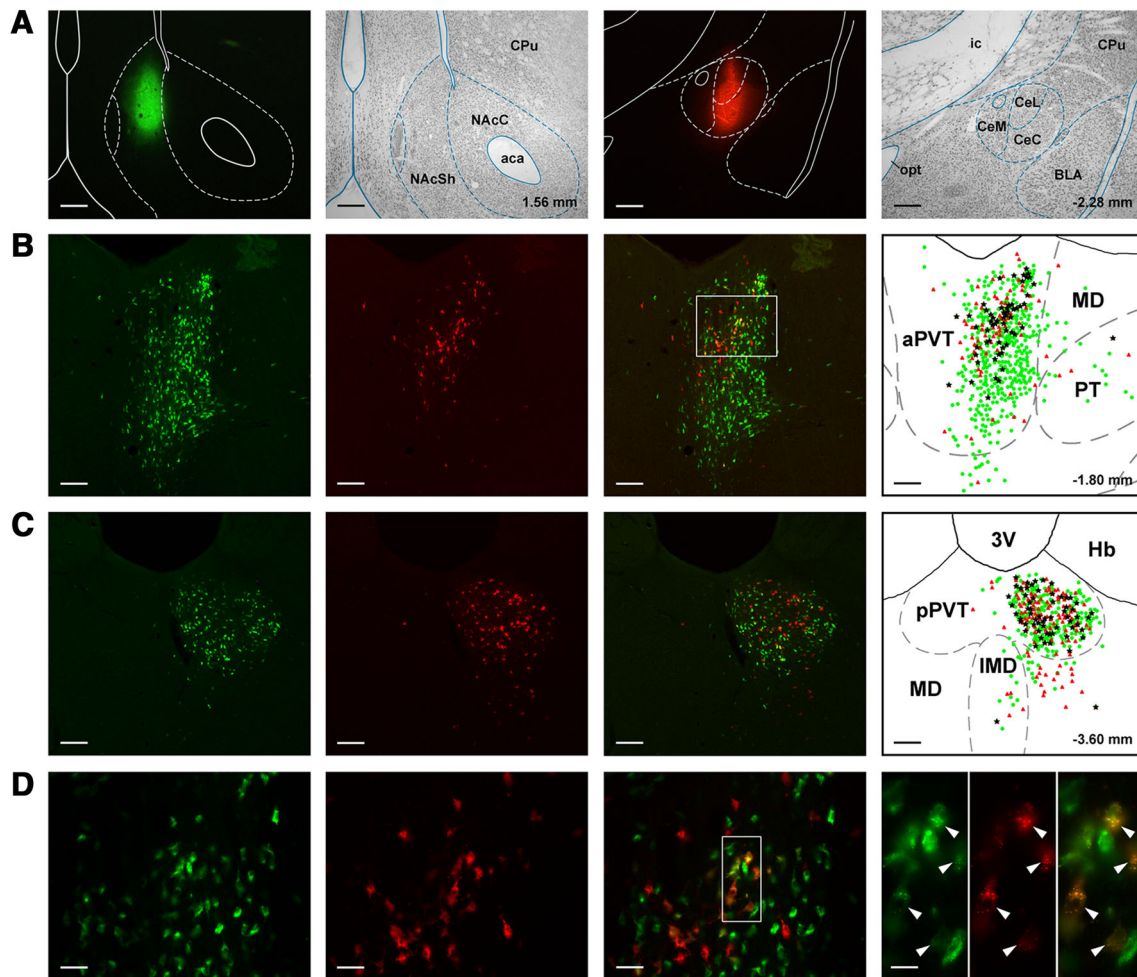
Fig. 1 *Images* and *drawings* of one representative case showing the tracer injection sites (**a**) in NAcSh (*green*) and CeL/CeC (*red*), and retrogradely labeled cells in aPVT (**b**) and pPVT (**c**) in coronal sections. **a** CTb injection sites with demarcation (*dashed line*) identified based on adjacent sections with NeuN staining. **b**, **c** *Images* of aPVT (**b**) and pPVT (**c**) section showing AF-CTb-488-labeled (*green*), AF-CTb-594-labeled (*red*) and double-labeled (*merged*; *yellow*) PVT neurons. *Drawing* of the same section on the *right* shows labeled neurons with demarcation of the midline thalamus adapted from a stereotaxic atlas (Paxinos and Watson 2009). Double-labeled neurons are identified as *black asterisk* in the *drawing*. Each *symbol* represents the position of a single neuron and the *numbers* at the *bottom* of each *picture* represent the approximate distance from bregma. **d** High magnification *images* of the same aPVT section in **b** (*white frame*) showing single- and double-labeled cells of the aPVT, the *inset* shown in the *last panel* was taken at a higher magnification. The *arrowheads* point to the double-labeled cells. For abbreviations, see list. *Scale bars* **a** 250 μm; **b**, **c** 100 μm; **d** 25 μm and the *inset* 10 μm

The purpose of this study is to provide a map of the location and an estimation of the number of neurons in the PVT that project to two different subcortical targets. The distributions of retrogradely labeled cells (single- and double-labeled neurons) are shown in four anterior–posterior levels of the PVT (Figs. 4, 5, 7). The proportion of labeled cells was estimated from the number of NeuN-stained neurons counted on the same levels used to count the fluorescent labeled neurons (Fig. 3). The average numbers of NeuN-stained neurons for the aPVT (7412 ± 379) and pPVT (5854 ± 274) were applied to all cases to estimate the proportion of CTb-labeled cells in the PVT that project to the different subcortical targets.

Combined injections into the NAcSh and CeL/CeC

The dense cores of the injection were located in the medial portion of the NAcSh and the CeL/CeC (Fig. 2). Figure 1 shows the anterior–posterior retrograde labeling observed in one representative case (Fig. 2, first case of the left column). The NAcSh-projecting cells were located throughout the PVT on the ipsilateral side of the injection (Figs. 1, 4a). Labeled cells were also found in other midline and intralaminar nuclei, including the paratenial (PT), paracentral (PC), and more sparsely in the central medial (CM), mediodorsal (MD) and intermediodorsal (IMD) thalamic nuclei. The CeL/CeC-projecting cells were
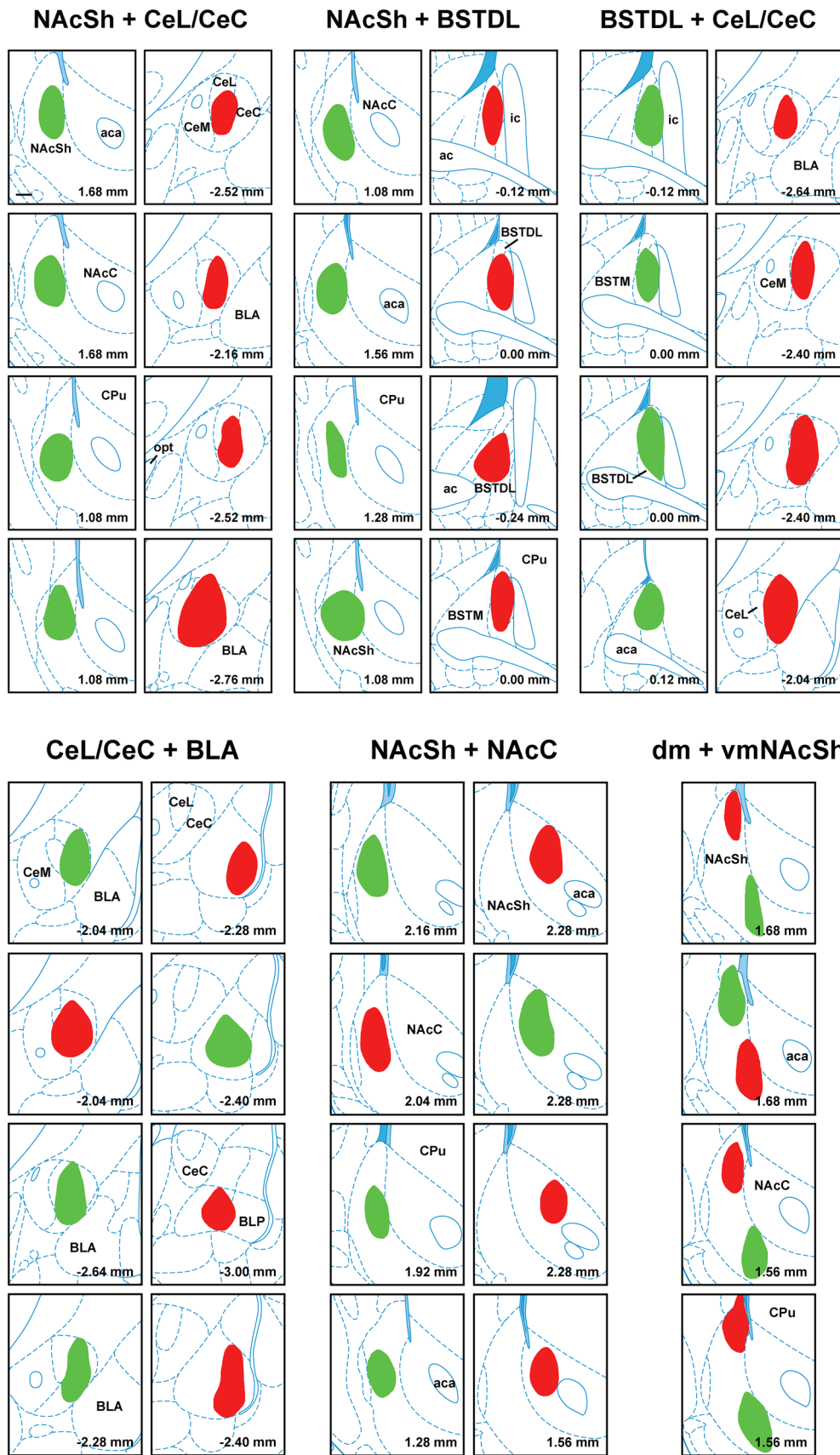
◀ **Fig. 2** Schematic representations of paired AF-CTb-488 (*green*) and AF-CTb-594 (*red*) injection sites in different cases. Injections were grouped as NAcSh + CeL/CeC; NAcSh + BSTDL; BSTDL + CeL/CeC; CeL/CeC + BLA; NAcSh + NAcC, and dmNAcSh + vmNAcSh. *Numbers* at the *bottom* of each *drawing* represent the approximate distance from bregma. For abbreviations, see list. *Scale bar* 250 μm

distributed sporadically in the more anterior sections of the PVT, but progressively increased in more posterior sections to numbers that are comparable to that of the NAcSh-projecting cells. The estimated percentages of single- and double-labeled cells in the aPVT and the pPVT for this case are shown in the lower right corner of Fig. 4a while the average proportions for the four cases are shown in Fig. 8a. Significantly more neurons in the aPVT projected to the NAcSh compared to the numbers of neurons projecting to the CeL/CeC ($F_{1,3} = 16.68$, $p = 0.027$; Fig. 8a). In contrast, there was no difference in the proportions of the pPVT neurons that projected to these two areas ($F_{1,3} = 0.94$, $p = 0.405$; Fig. 8a). A proportion of cells was found to project to both the NAcSh and the CeL/CeC with 7.0 and 8.6% of the total number of neurons in aPVT and pPVT, respectively. It is noteworthy that nearly half of the aPVT neurons that projected to the CeL/CeC also projected to the NAcSh, whereas approximately 30% of the

pPVT neurons that projected to the CeL/CeC projected to the NAcSh (Fig. 8a). Finally, the one case that involved a larger injection of CTb in the CeL/CeC (100 nl, last case in Fig. 2 left column) produced more labeled cells in the PVT, but the pattern of distribution and the proportion of doubled-labeled cells remained similar to the other cases (data not shown).

Combined injections into the NAcSh and BSTDL

The BSTDL- and NAcSh-projecting cells were distributed throughout the dorsal–ventral and anterior–posterior extent of the PVT (Fig. 4b). A large number of BSTDL-projecting cells were also found in other midline thalamic nuclei. More neurons in the aPVT projected to the NAcSh compared to the numbers of neurons projecting to the BSTDL ($F_{1,3} = 181.98$, $p = 0.001$; Fig. 8b). However, there was no difference in the proportions of the pPVT neurons that projected to these two areas ($F_{1,3} = 8.03$, $p = 0.066$; Fig. 8b). A proportion of cells was found to project to both the NAcSh and the BSTDL with 16.0 and 17.4% of the total number of neurons in aPVT and pPVT, respectively. In this combination, almost a half of the BSTDL-projecting cells were found to also project to the NAcSh (Fig. 8b). It is clear from a qualitative perspective that a larger proportion of NAcSh-projecting cells also projected to the

Fig. 3 **a** *Images* showing the location of the aPVT and pPVT in the midline thalamus immunoreacted for NeuN. **b** Numbers of NeuN-stained cells at different anterior–posterior levels of the PVT. Cells were counted bilaterally at 16 levels (1–16, anterior to posterior) in four animals. Values are shown as mean ± SEM in **b**. For abbreviations, see list. *Scale bar* 250 μm
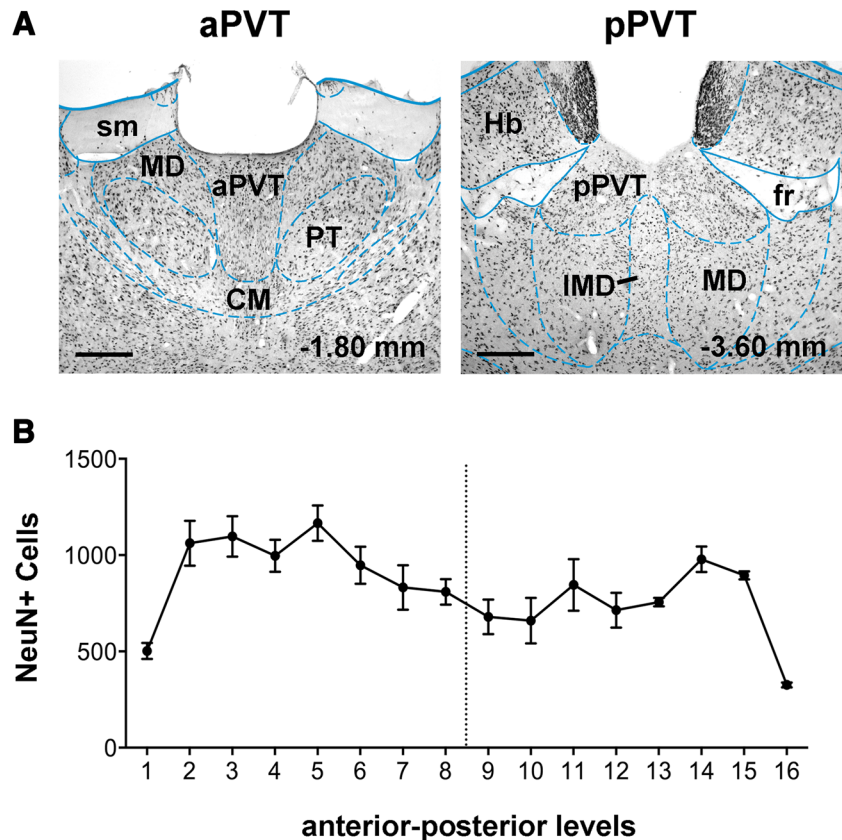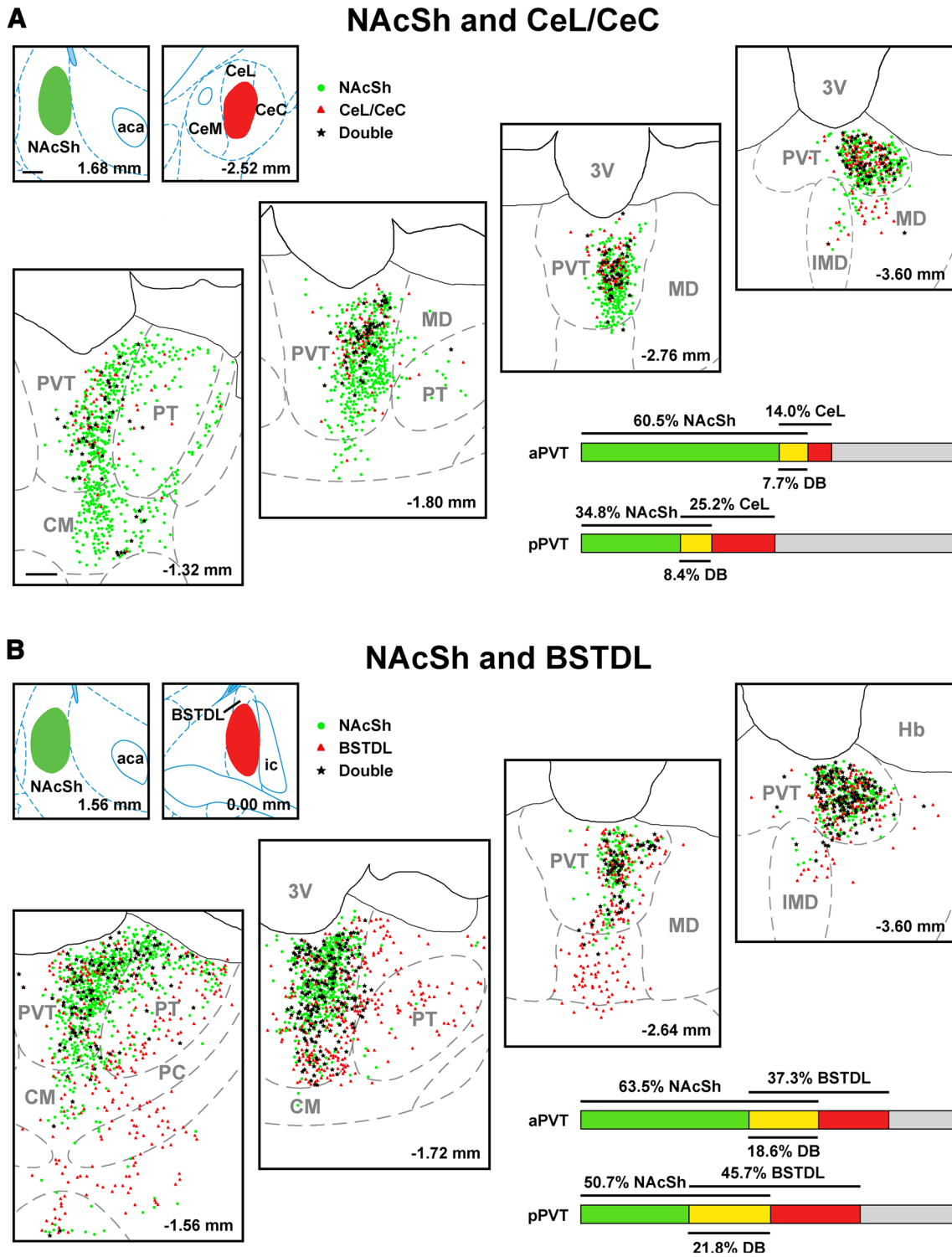
Fig. 4 a A representative case with combined injections in the NAcSh (*green*) and CeL/CeC (*red*). *Drawings* of labeled cells are from four anterior–posterior levels with the approximate distance from bregma shown as *numbers* at the *bottom* of each *drawing*. Cells projecting to the NAcSh are in *green* (*dot*), CeL/CeC are in *red* (*triangle*), and the double-labeled neurons are in *black* (*asterisk*). Each *symbol* represents the position of a single neuron and the *numbers* at the *bottom* of each picture represent the approximate distance from bregma. The estimated percentages of single- and double-labeled (*DB*) neurons to the total number of NeuN+ cells in the aPVT vs the pPVT are shown in the *bar graphs* at the *lower right corner*. **b** A case with combined injections in the NAcSh (*green*) and BSTDL (*red*). For other abbreviations, see list. *Scale bars* 250 μm for injection sites, 150 μm for *drawings*

BSTDL (aPVT 28%, pPVT 40%) than to the CeL/CeC (aPVT 14%, pPVT 22%).

Combined injections into the BSTDL and CeL/CeC

The distribution of BSTDL-projecting cells (Figs. 5a, 6) was comparable to the previous combination (Fig. 4b) with large numbers of cells found throughout the anterior to posterior extent of the PVT and surrounding nuclei in the midline thalamus. The pattern of CeL/CeC-projecting cells (Figs. 5a, 6) was also similar to the case in Fig. 4a with labeled cells being largely confined to the PVT. No difference was found in the proportions of neurons that projected to these two areas at either aPVT ($F_{1,3} = 8.26$, $p = 0.064$; Fig. 8c) or pPVT ($F_{1,3} = 1.74$, $p = 0.279$; Fig. 8c). The proportion of double-labeled cells projecting to both the BSTDL and CeL/CeC was 5.9 and 12.5% of the total number of neurons in aPVT and pPVT, respectively.

Combined injections into the CeL/CeC and BLA

The distribution of CeL/CeC-projecting cells in this combination (Fig. 5b) was similar to the case shown in Fig. 4a. The BLA-projecting cells were scattered in the more anterior sections of the PVT and other midline thalamic nuclei while their numbers progressively increased in more posterior sections of the PVT in a pattern that was similar to the CeL/CeC-projecting cells in the pPVT. The CeL/CeC- and BLA-projecting cells were largely intermingled throughout the PVT region and there was no appearance of topographical segregation of subpopulation that was projection specific for CeL/CeC or BLA. There was significantly more CeL/CeC-projecting neurons than BLA-projecting neurons in both aPVT ($F_{1,3} = 10.67$, $p = 0.047$; Fig. 8d) and pPVT ($F_{1,3} = 17.39$, $p = 0.025$; Fig. 8d). The proportion of double-labeled cells projecting to both the CeL/CeC and BLA was 1.9 and 7.1% of the total number of neurons in aPVT and pPVT, respectively.

Combined injections into the NAcSh and NAcC

The NAcC-projecting cells were found throughout the anterior–posterior extent of the PVT and intermingled with shell-projecting cells (Fig. 7a). The number of labeled NAcC-projecting PVT cells was lower than the NAcSh-projecting cells while more core-projecting cells were found in PT, PC, CM, and IMD. The core-projecting cells were found more in the lateral and ventral part of the PVT when compared to shell-projecting cells. More neurons in the aPVT were found to project to the shell compared to neurons projecting to the core ($F_{1,3} = 26.89$, $p = 0.014$; Fig. 8e). No difference was found in the proportions of the pPVT neurons that projected to these two areas

($F_{1,3} = 0.85$, $p = 0.428$; Fig. 8e). A proportion of cells was found to project to both the shell and core with 15.8 and 13.9% of the total number of neurons in aPVT and pPVT, respectively. However, it should be pointed out that 38–49% of the neurons that were found to project to the core were also found to project to the shell.

Combined injections into the vmNAcSh and dmNAcSh

The distribution of vmNAcSh-projecting cells in the midline thalamus was different from the pattern of dmNAcSh-projecting cells (Fig. 7b). The posterior levels of the PVT contained a larger number of vmNAcSh-projecting cells than anterior-most sections of the PVT. In fact, the pPVT contained more vmNAcSh-labeled cells than it did following injection of the tracer in the medial shell (see Figs. 4a, b, 7a). There were also a relatively large number of vmNAcSh-projecting cells in the PT and PC. The dmNAcSh-projecting cells were found throughout the dorsoventral extent of the aPVT, whereas fewer of these projection-specific cells were found in the pPVT where they were mostly located in the dorsal most region of the pPVT. Few dmNAcSh-projecting cells were found in other midline thalamic nuclei. There was no difference in the proportions of the aPVT neurons that project to dmNAcSh or vmNAcSh ($F_{1,3} = 0.63$, $p = 0.485$; Fig. 8f), but more neurons in the pPVT projected to the vmNAcSh ($F_{1,3} = 34.26$, $p = 0.010$; Fig. 8f). A relatively small proportion of PVT neurons was found to project to both the vmNAcSh and the dmNAcSh (10.3 and 7.5% of the total number of neurons in aPVT and pPVT, respectively).

Discussion

The present study describes the projections from the PVT to the NAcSh, NAcC, BSTDL and amygdala using a dual retrograde tracing method. A key finding is that most neurons in the PVT appear to innervate the NAc and that a significant portion of these NAc-projecting neurons give off collaterals to innervate a variety of subcortical targets including the BSTDL and CeL/CeC. The study suggests that most neurons in the PVT exert an extensive influence on the NAc, and that at the same time these neurons also likely exert a broad influence on a large continuum of subcortical structures. Along the same line, differences in the pattern of projections from the aPVT and pPVT are suggestive of potential functional differences in terms of its ability to bias afferent activity to different regions of the NAcSh in addition to the BSTDL and CeL/CeC.

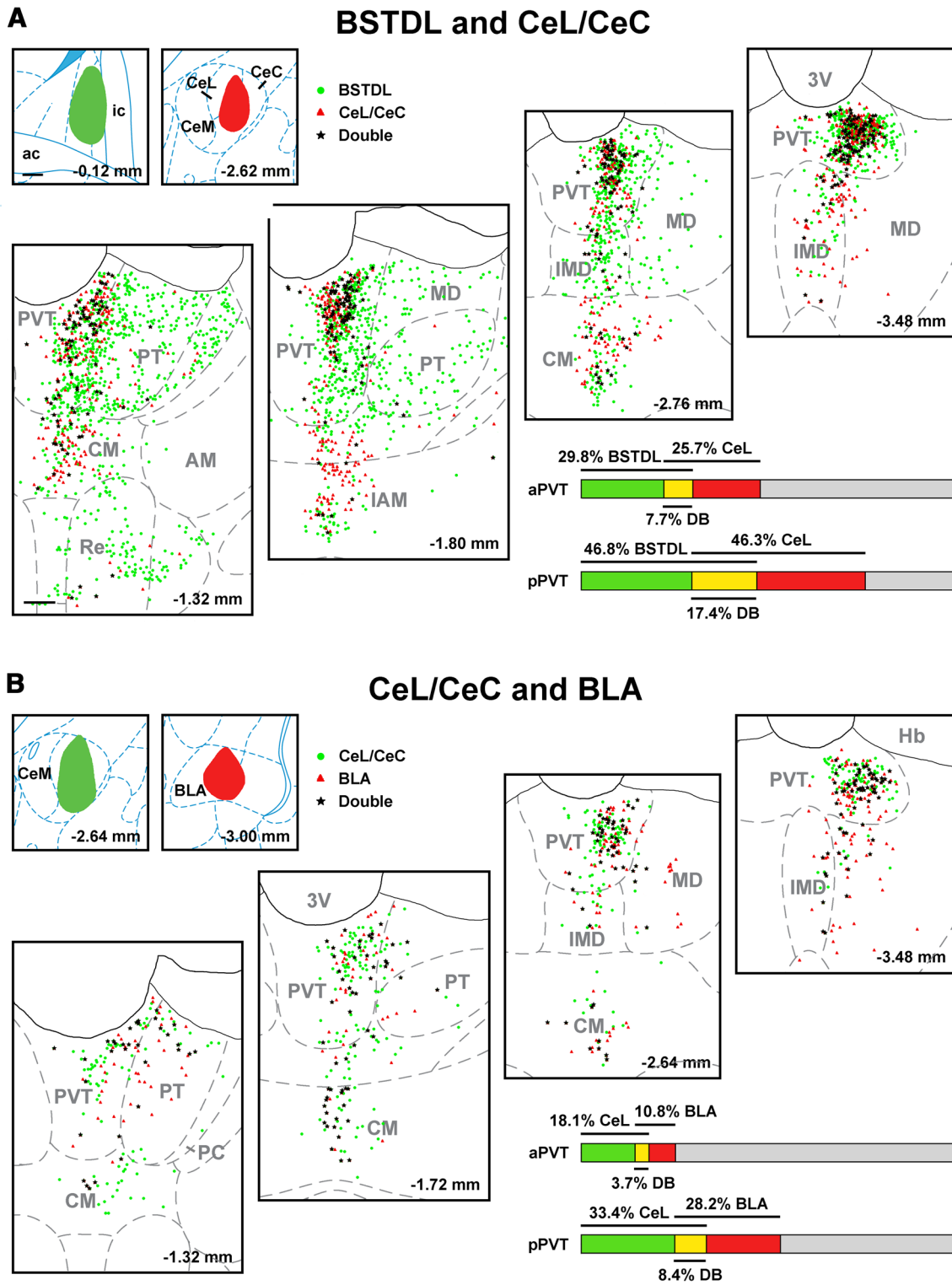We observed a moderate level of collateralization in the projections from the PVT to the NAcSh, NAcC, BSTDL,

Fig. 5 a A representative case with combined injections in the BSTDL (*green*) and CeL/CeC (*red*). Cells projecting to the BSTDL are in *green* (*dot*), CeL/CeC are in *red* (*triangle*), and the double-labeled neurons are in *black* (*asterisk*). Each *symbol* represents the position of a single neuron and the *numbers* at the *bottom* of each *picture* represent the approximate distance from bregma. The estimated percentages of single- and double-labeled neuron to the total number of NeuN+ cells in the aPVT vs the pPVT are shown in the *bar graphs* at the *lower right corner*. **b** A case with combined injections in the CeL/CeC (*green*) and BLA (*red*). For other abbreviations, see list. *Scale bars* 250 μm for injection sites, 150 μm for *drawings*
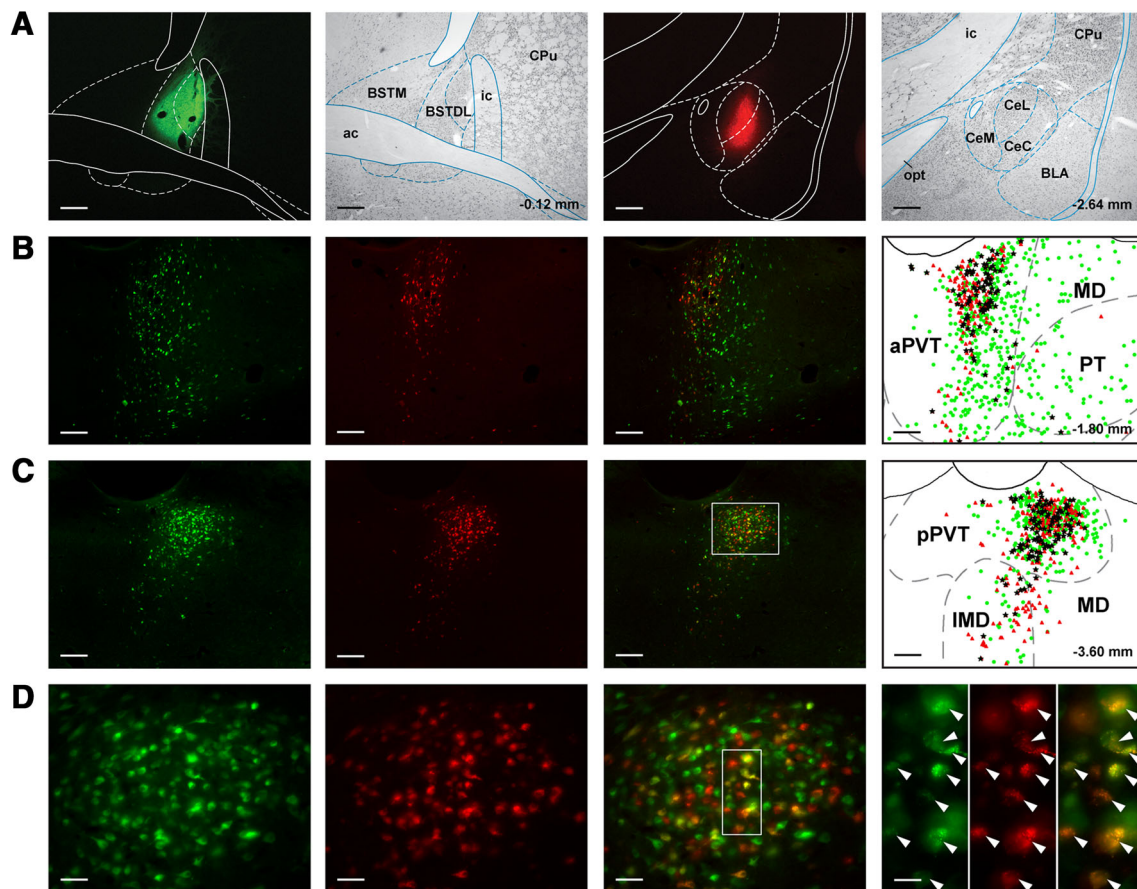
Fig. 6 *Images* and *drawings* of one representative case showing the tracer injection sites (**a**) in BSTDL (*green*) and CeL/CeC (*red*), and retrogradely labeled cells in aPVT (**b**) and pPVT (**c**) in coronal sections. **a** CTb injection sites with demarcation (*dashed line*) identified based on adjacent sections with NeuN staining. **b, c** *Images* of aPVT (**b**) and pPVT (**c**) section showing AF-CTb-488-labeled (*green*), AF-CTb-594-labeled (*red*) and double-labeled (merged; *yellow*) PVT neurons. *Drawing* of the same section on the *right* shows labeled neurons with demarcation of the midline thalamus adapted from a stereotaxic atlas (Paxinos and Watson 2009). Double-labeled neurons are identified as *black asterisk* in the *drawing*. Each *symbol* represents the position of a single neuron and the *numbers* at the *bottom* of each *picture* represent the approximate distance from bregma. **d** High magnification *images* of the same pPVT section in **c** (*white frame*) showing single- and double-labeled cells of the pPVT, the inset shown in the *last panel* was taken at a higher magnification. The *arrowheads* point to the double-labeled cells. For abbreviations, see list. *Scale bars* **a** 250 μm; **b, c** 100 μm; **d** 25 μm, inset 10 μm

and CeL/CeC. It should be understood that the approach used in the present study would likely generate an underestimation of the extent of collateralization, because the comparison made was between two small injections involving limited portions of the large region of subcortical tissue innervated by the PVT that extends from the anterior pole of the nucleus accumbens to the CeA (Li and Kirouac 2008). Another important point to consider is that largely separate populations of the neurons in the PVT were labeled when injections were made in the dmNAcSh and vmNAcSh despite labeling up to 80% of the neurons in the PVT. Consequently, it is very likely that the number of neurons that project to both the NAc and other subcortical areas like the BSTDL and CeL/CeC would be much greater than seen with the combination injections made in this study. Consistent with this view, a recent single cell reconstruction study also reported that all of the neurons

traced from the PVT collateralized in the NAcSh and provided variable amount of collaterals to a number of subcortical targets including the BSTDL and CeA (Unzai et al. 2017).

The neurons that projected to the different subcortical targets were found to be intermixed in the PVT and did not form distinct clusters of neurons. A number of studies have reported that the neurons in the PVT that project to the NAc were different from the neurons that project to the prefrontal cortex, ventral subiculum of the hippocampus and the basolateral amygdala (Bubser and Deutch 1998; Shinonaga et al. 1994; Su and Bentivoglio 1990). Neurons that project to the CeL and BLA were also reported to be segregated in distinctive clusters of neurons in the pPVT (Penzo et al. 2015). In contrast, another study reported a high level of collateralization in PVT neurons that project to the prelimbic cortex and NAc (Otake and Nakamura
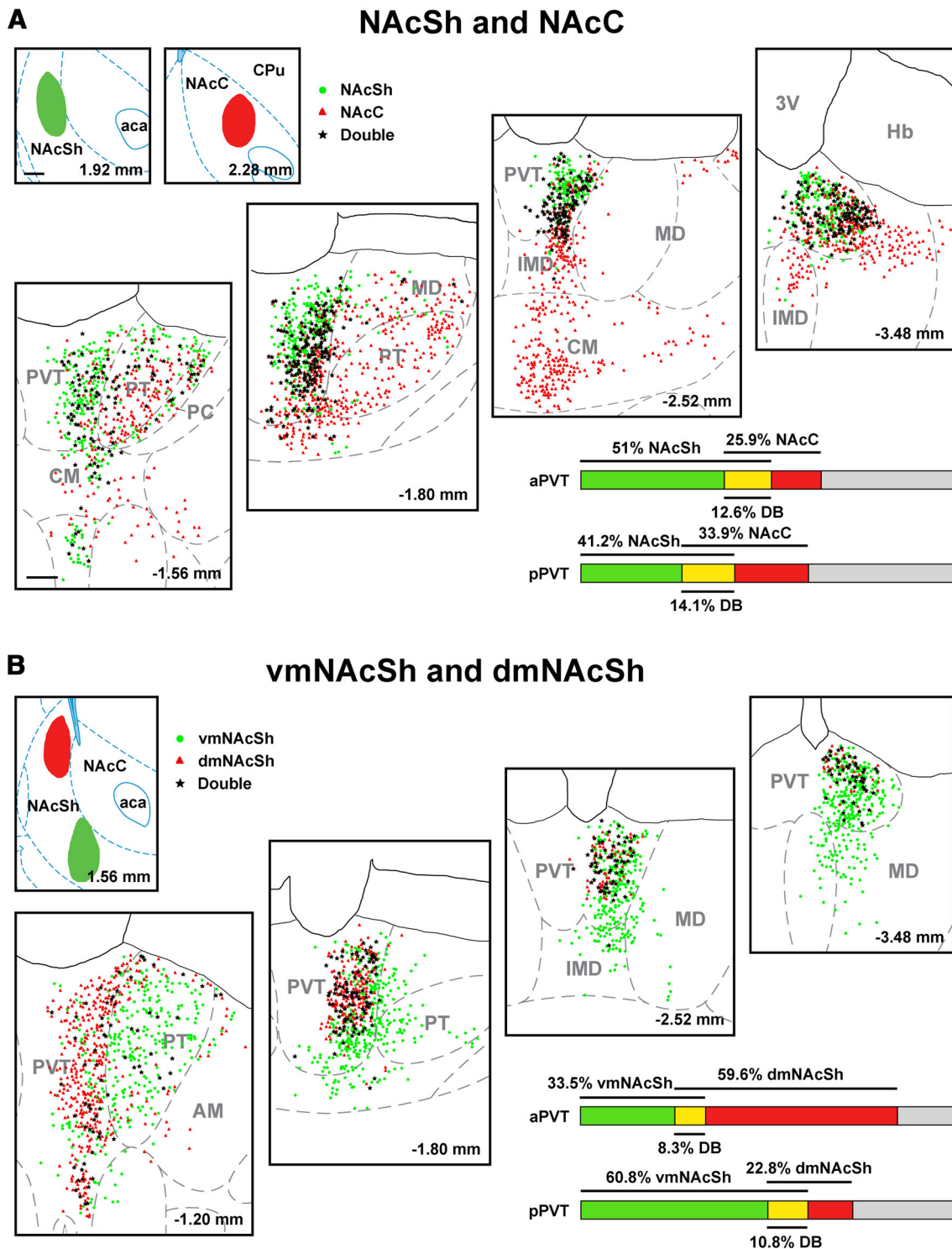
Fig. 7 **a** A representative case with combined injections in the NAcSh (*green*) and NAcC (*red*). Cells projecting to the NAcSh are in *green* (*dot*), NAcC are in *red* (*triangle*), and double-labeled neurons are in *black* (*asterisk*). Each *symbol* represents the position of a single neuron and the *numbers* at the *bottom* of each picture represent the approximate distance from bregma. The estimated percentages of single- and double-labeled neuron to the total number of NeuN+ cells in the aPVT vs the pPVT are shown in the *bar graphs* at the *lower right corner*. **b** A case with combined injections in the vmNAcSh (*green*) and dmNAcSh (*red*). For other abbreviations, see list. *Scale bars* 250 μm for injection sites, 150 μm for *drawings*
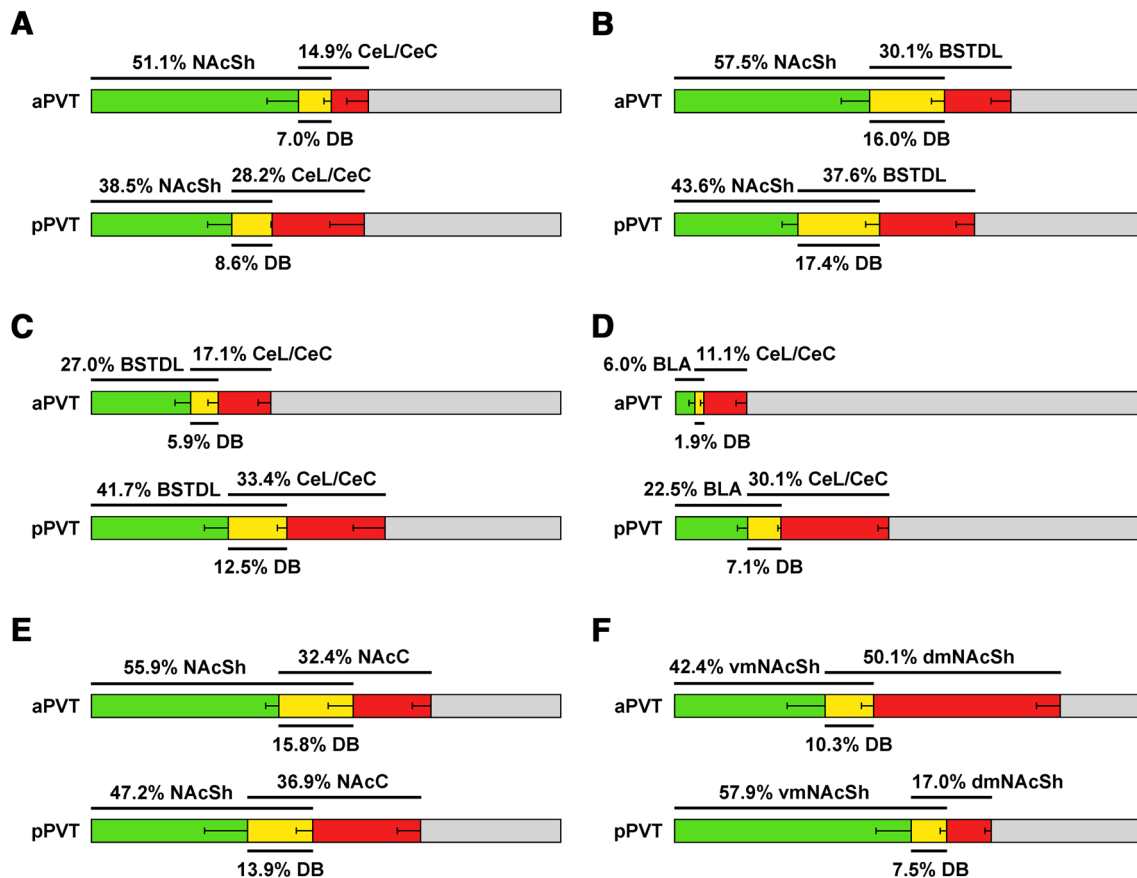
Fig. 8 The average proportions of single- and double-labeled neurons in the aPVT and pPVT in all six injection combinations ($n = 4$). **a** NAcSh + CeL/CeC; **b** NAcSh + BSTDL; **c** CeL/CeC + BSTDL; **d** CeL/CeC + BLA; **e** NAcSh + NAcC; **f** dmNAcSh + vmNAcSh.

Values are shown as mean $-$ SEM. *Error bars* represent the SEMs of the proportions of the PVT neurons that project to one of the injection sites or both. *DB* double-labeled. For other abbreviations, see list

1998). The high level of fiber collateralization described in this paper compared to some previous papers is likely due to the fact that the injections of the retrograde tracer in the present study were placed in subcortical regions that receive the heaviest PVT innervation and not to cortical or cortical-like structures like the prefrontal cortex, subiculum, and basolateral amygdala (Bubser and Deutch 1998; Shinonaga et al. 1994; Su and Bentivoglio 1990) which are innervated significantly less densely than the NAcSh, BSTDL and CeL/CeC (Li and Kirouac 2008). This may also be in part due to the fact that PVT fibers give off more collaterals and with dense collections of fiber terminals in subcortical regions than in the cortex (Unzai et al. 2017).

It is evident from the present study as well as other anterograde tracing experiments that the NAc is the major output target of the PVT (Li and Kirouac 2008; Vertes and Hoover 2008). For instance, we consistently found that nearly 50% of the neurons in the PVT were labeled following injections of the CTb within a relatively small portion of the NAcSh. Indeed, nearly 80% of the neurons in the PVT on the sections counted were retrogradely labeled

when injections of CTb involved a portion of the dmNAcSh and vmNAcSh. This is consistent with a previous anterograde tracing study that showed that a small injection of biotin dextran amine (BDA) in a restricted region of the PVT produced very dense fiber labeling throughout the NAcSh (Li and Kirouac 2008). This suggests that most neurons in the PVT provide axonal fibers that bifurcate extensively through most of the NAc. In support of this, a single cell reconstruction study reported that PVT neurons give off collaterals throughout large portions of the NAc before reaching the prefrontal cortex (Unzai et al. 2017).

It was somewhat unexpected that the number of double-labeled cells in the cases with combined injections in the dmNAcSh and vmNAcSh was relatively low (<10%) considering that the combination resulted in up to 80% of all the cells in the PVT being labeled by these two injections. The location of the cells innervating the dmNAcSh and vmNAcSh was for the most part distributed throughout the PVT. However, there were some notable topographical differences. For example, the anterior-most sections of the

PVT contained a large number of dmNAcSh-projecting cells. There was a progressive decrease in the number of dmNAcSh-projecting cells in the most posterior levels of the PVT with these cells occupying the dorsal region of the pPVT. This distribution is consistent with a previous report with a retrograde tracer injection in the septal pole of the NAcSh (Bubser and Deutch 1998). The number and location of vmNAcSh-projecting cells in the PVT displayed an arrangement opposite to the dmNAcSh-projecting cells with more vmNAcSh-projecting cells localized in the ventral region of the more posterior sections of the PVT. The overall pattern is consistent with a previous anterograde study which showed that the aPVT provides a dense input to the dmNAcSh, while the pPVT preferentially innervates the vmNAcSh (Li and Kirouac 2008). The location of the NAcC-projecting cells was also topographically organized in the PVT with NAcC-projecting cells found in greater numbers in the more lateral aspects of the PVT as well as areas lateral and ventral to the PVT (PT, CM, and IMD). However, there were no apparent differences in the total number of single- or double-labeled neurons in the aPVT and pPVT following injections of CTb in the NAcC. The general pattern of labeling observed in the midline thalamus following injections of the retrograde tracer CTb reported here is consistent with previous anterograde tracing studies (Berendse and Groenewegen 1990; Li and Kirouac 2008; Vertes and Hoover 2008) which is summarized as follows. First, the dmNAcSh is preferentially innervated by the anterior-most levels of the PVT, while the vmNAcSh is preferentially innervated by the more posterior levels (Li and Kirouac 2008). Second, the NAcC receives strong projections from the PVT, intermediodorsal and central medial nuclei (Berendse and Groenewegen 1990; Li and Kirouac 2008; Vertes and Hoover 2008). Third, the paratenial nucleus provides a strong innervation of the NAcC and NAcSh in a pattern that resembles that of the PVT (Berendse and Groenewegen 1990; Vertes and Hoover 2008).

Methodological considerations

Cholera toxin B can be picked up by intact fibers-of-passage and some caution is required when interpreting results using tracing substances like CTb (Chen and Aston-Jones 1995). The present study used glass micropipettes to slowly inject low volumes of CTb to minimize the possibility that the injection procedure would cause damaged axonal fibers and retrograde labeling through these damaged fibers. While the micropipette will invariably cause some damage to the brain tissue above the injection sites, we were unable to find instances of false labeling of neurons that project to the areas studied. For example, injections in the BSTDL or CeL/CeC may produce labeling via fibers passing through

these areas. However, injections that were off-target in the medial BST or medial CeA had much fewer labeled neurons in the PVT indicating that was not likely the case (data not shown). In addition, the pattern of labeling observed in the PVT in the present study was similar to a previous study in which CTb was iontophoretically applied with finer micropipettes (Li and Kirouac 2008). The low proportion of double-labeled cells in cases with dmNAcSh and vmNAcSh injections also indicates that uptake by fibers-of-passage was not an issue.

The use of the same tracer substance for the two injections is also an important advantage in that the injections would have given rise to labeled cells from mechanisms involving similar efficiency of uptake and transport. The only study that we are aware of, albeit limited in scope and not quantitative in nature, reported comparable retrograde labeling from the 488 and 594 conjugates (Conte et al. 2009). We also found in combinations where we reversed the location of the two conjugates led to a similar number of labeled neurons in the PVT. However, it is possible that one tracer is more efficient than the other which could yield an underestimation of the proportion of double-labeled neurons.

Functional considerations

The present study demonstrates that most of the neurons in the PVT project to NAc while at the same time sending collaterals to other subcortical targets like the BSTDL and CeL/CeC. This observation suggests that an increase in the activity of neurons in the PVT may exert a global influence on a number of basal forebrain structures. Recent studies using optogenetic and chemogenetic approaches showed that the PVT may modulate behavior in a projection-specific manner. For example, manipulations that selectively targeted PVT fibers in the CeL were shown to modulate fear learning and retrieval of conditioned fear memory (Do-Monte et al. 2015; Penzo et al. 2015). In other studies, optogenetic activation of PVT fibers to the NAcSh was shown to promote sucrose-seeking behavior (Labouebe et al. 2016) or to produce an aversive state (Zhu et al. 2016). Considering the extent of collateralization of PVT fibers to the NAcSh and CeL/CeC, experimental manipulations of a single projection target of the PVT will likely provide only a partial assessment of the type of influence the PVT would have on the neural circuits that control behavior. A more likely scenario would be one where PVT afferents to different subcortical regions would serve to coordinate a cohesive behavioral response to complex situations and competing motivational states. For example, a situation involving fear might require an organism to become immobile through mechanisms involving the CeL while other neural circuits in the NAc

and BST might be recruited to modulate competing (exploration, food intake, sex) or supportive (avoidance, flight, fight) behaviors. In this example, recruitment of a group of neurons in the PVT could support the behavioral response associated with fear via the projection to the CeL (Do-Monte et al. 2015; Penzo et al. 2015) while at the same time engaging circuits in the NAc and BST that mediate anxiety and avoidance (Zhu et al. 2016). It is also possible that activation of PVT collaterals could have contrasting effects on behaviors with different emotional valences. An example of this would be a scenario where fear would cause activation of the PVT fibers to the CeL that mediate immobility (Do-Monte et al. 2015; Penzo et al. 2015) while at the same time activating fibers in the NAcSh that suppress food seeking and intake (Stratford and Wirtshafter 2013). Support for this coordinating role for the PVT is provided by recent evidence showing that the presence of competing aversive and appetitive motivational state determines how the PVT influences behavior (Choi and McNally 2017; Do-Monte et al. 2017).

The present study also showed that the dmNAcSh was preferentially innervated by the aPVT while the vmNAcSh and the CeL/CeC were preferentially innervated by the pPVT. This is in line with a previous anterograde tracing study that showed a similar pattern of innervation by the aPVT and pPVT (Li and Kirouac 2008). This pattern of innervation may suggest potential functional differences between the aPVT and the pPVT. For instance, the dmNAcSh has been implicated in appetitive and reward-related behaviors (Pecina et al. 2006; Reed et al. 2015) and may represent a specialized role for the aPVT in behaviors with a positive emotional valence. In support of this, the neuropeptides orexin and substance P were shown to increase ethanol intake through pharmacological actions at the aPVT that were not present in the pPVT (Barson et al. 2015, 2017). In contrast, the CeL and the BSTDL have been implicated in avoidance and defensive behaviors (Davis et al. 2010; LeDoux 2000) and pPVT projections to these areas may represent a means for the PVT to influence behaviors with a negative emotional valence as indicated by a number of studies (Barson and Leibowitz 2015; Do-Monte et al. 2015; Dong et al. 2015; Heydendael et al. 2011; Li et al. 2009, 2010a, b, 2011, 2014; Penzo et al. 2015). The posterior half of the NAcSh has been implicated in defensive behaviors (Berridge and Kringelbach 2015; Reynolds and Berridge 2008) and may represent a means by which a projection from the pPVT to vmNAcSh could also contribute to negative emotional behaviors. Consequently, a strong activation of the aPVT may bias behaviors related to positive emotional states, whereas strong activation of the pPVT may bias behaviors related to negative emotional states. Finally, we speculate that the relatively high level of collateralization in the projections of the PVT suggests that this area of the

thalamus modulates a general aspect of appetitive and aversive behaviors, for example, the arousal, vigilance, or attention aspects necessary for a behavioral response. This is in consonance with the functional role of other midline thalamic nuclei in these brain functions (Smith et al. 2004; Van der Werf et al. 2002).

References

Barson JR, Leibowitz SF (2015) GABA-induced inactivation of dorsal midline thalamic subregions has distinct effects on emotional behaviors. Neurosci Lett 609:92–96. doi:10.1016/j.neulet.2015.10.029

Barson JR, Ho HT, Leibowitz SF (2015) Anterior thalamic paraventricular nucleus is involved in intermittent access ethanol drinking: role of orexin receptor 2. Addict Biol 20:469–481. doi:10.1111/adb.12139

Barson JR, Poon K, Ho HT, Alam MI, Sanzalone L, Leibowitz SF (2017) Substance P in the anterior thalamic paraventricular nucleus: promotion of ethanol drinking in response to orexin from the hypothalamus. Addict Biol 22:58–69. doi:10.1111/adb.12288

Bentivoglio M, Balercia G, Kruger L (1991) The specificity of the nonspecific thalamus: the midline nuclei. Prog Brain Res 87:53–80

Berendse HW, Groenewegen HJ (1990) Organization of the thalamostriatal projections in the rat, with special emphasis on the ventral striatum. J Comp Neurol 299:187–228

Berridge KC, Kringelbach ML (2015) Pleasure systems in the brain. Neuron 86:646–664. doi:10.1016/j.neuron.2015.02.018

Browning JR, Jansen HT, Sorg BA (2014) Inactivation of the paraventricular thalamus abolishes the expression of cocaine conditioned place preference in rats. Drug Alcohol Depend 134:387–390. doi:10.1016/j.drugalcdep.2013.09.021

Bubser M, Deutch AY (1998) Thalamic paraventricular nucleus neurons collateralize to innervate the prefrontal cortex and nucleus accumbens. Brain Res 787:304–310

Chen S, Aston-Jones G (1995) Evidence that cholera toxin B subunit (CTb) can be avidly taken up and transported by fibers of passage. Brain Res 674:107–111

Choi E, McNally G (2017) Paraventricular thalamus balances danger and reward. J Neurosci 37:3018–3029. doi:10.1523/JNEUROSCI.3320-16.2017

Choi DL, Davis JF, Fitzgerald ME, Benoit SC (2010) The role of orexin-A in food motivation, reward-based feeding behavior and food-induced neuronal activation in rats. Neuroscience 167:11–20. doi:10.1016/j.neuroscience.2010.02.002

Conte WL, Kamishina H, Reep RL (2009) The efficacy of the fluorescent conjugates of cholera toxin subunit B for multiple retrograde tract tracing in the central nervous system. Brain Struct Funct 213:367–373. doi:10.1007/s00429-009-0212-x

Davis M, Walker DL, Miles L, Grillon C (2010) Phasic vs sustained fear in rats and humans: role of the extended amygdala in fear vs anxiety. Neuropsychopharmacology 35:105–135. doi:10.1038/npp.2009.109

Do-Monte FH, Quinones-Laracuente K, Quirk GJ (2015) A temporal shift in the circuits mediating retrieval of fear memory. Nature 519:460–463. doi:10.1038/nature14030

Do-Monte FH, Minier-Toribio AM, Quiñones-Laracuente K, Medina-Colón EM, Quirk GJ (2017) Thalamic regulation of sucrose seeking during unexpected reward omission. Neuron 94:388–400.e4. doi:10.1016/j.neuron.2017.03.036

Dong X, Li Y, Kirouac GJ (2015) Blocking of orexin receptors in the paraventricular nucleus of the thalamus has no effect on the expression of conditioned fear in rats. Front Behav Neurosci 9:161. doi:10.3389/fnbeh.2015.00161

Ehrlich I, Humeau Y, Grenier F, Ciocchi S, Herry C, Luthi A (2009) Amygdala inhibitory circuits and the control of fear memory. Neuron 62:757–771. doi:10.1016/j.neuron.2009.05.026

Floresco SB (2015) The nucleus accumbens: an interface between cognition, emotion, and action. Annu Rev Psychol 66:25–52. doi:10.1146/annurev-psych-010213-115159

Groenewegen HJ, Berendse HW (1994) The specificity of the 'nonspecific' midline and intralaminar thalamic nuclei. Trends Neurosci 17:52–57

Hamlin AS, Clemens KJ, Choi EA, McNally GP (2009) Paraventricular thalamus mediates context-induced reinstatement (renewal) of extinguished reward seeking. Eur J Neurosci 29:802–812

Heydendael W, Sharma K, Iyer V, Luz S, Piel D, Beck S, Bhatnagar S (2011) Orexins/hypocretins act in the posterior paraventricular thalamic nucleus during repeated stress to regulate facilitation to novel stress. Endocrinology 152:4738–4752. doi:10.1210/en.2011-1652

Hsu DT, Price JL (2009) Paraventricular thalamic nucleus: subcortical connections and innervation by serotonin, orexin, and corticotropin-releasing hormone in macaque monkeys. J Comp Neurol 512:825–848

Hsu DT, Kirouac GJ, Zubieta JK, Bhatnagar S (2014) Contributions of the paraventricular thalamic nucleus in the regulation of stress, motivation, and mood. Front Behav Neurosci 8:73. doi:10.3389/fnbeh.2014.00073

James MH et al (2010) Cocaine- and amphetamine-regulated transcript (CART) signaling within the paraventricular thalamus modulates cocaine-seeking behaviour. PLoS One 5:e12980. doi:10.1371/journal.pone.0012980

Kirouac GJ (2015) Placing the paraventricular nucleus of the thalamus within the brain circuits that control behavior. Neurosci Biobehav Rev 56:315–329. doi:10.1016/j.neubiorev.2015.08.005

Labouebe G, Boutrel B, Tarussio D, Thorens B (2016) Glucose-responsive neurons of the paraventricular thalamus control sucrose-seeking behavior. Nat Neurosci 19:999–1002. doi:10.1038/nn.4331

LeDoux JE (2000) Emotion circuits in the brain. Annu Rev Neurosci 23:155–184. doi:10.1146/annurev.neuro.23.1.155

Li S, Kirouac GJ (2008) Projections from the paraventricular nucleus of the thalamus to the forebrain, with special emphasis on the extended amygdala. J Comp Neurol 506:263–287

Li Y, Li S, Sui N, Kirouac GJ (2009) Orexin-A acts on the paraventricular nucleus of the midline thalamus to inhibit locomotor activity in rats. Pharmacol Biochem Behav 93:506–514

Li Y, Li S, Wei C, Wang H, Sui N, Kirouac GJ (2010a) Changes in emotional behavior produced by orexin microinjections in the paraventricular nucleus of the thalamus. Pharmacol Biochem Behav 95:121–128

Li Y, Li S, Wei C, Wang H, Sui N, Kirouac GJ (2010b) Orexins in the paraventricular nucleus of the thalamus mediate anxiety-like responses in rats. Psychopharmacology 212:251–265. doi:10.1007/s00213-010-1948-y

Li Y, Wang H, Qi K, Chen X, Li S, Sui N, Kirouac GJ (2011) Orexins in the midline thalamus are involved in the expression of conditioned place aversion to morphine withdrawal. Physiol Behav 102:42–50. doi:10.1016/j.physbeh.2010.10.006

Li Y, Dong X, Li S, Kirouac GJ (2014) Lesions of the posterior paraventricular nucleus of the thalamus attenuate fear expression. Front Behav Neurosci 8:94. doi:10.3389/fnbeh.2014.00094

Luppi PH, Fort P, Jouvet M (1990) Iontophoretic application of unconjugated cholera toxin B subunit (CTb) combined with immunohistochemistry of neurochemical substances: a method for transmitter identification of retrogradely labeled neurons. Brain Res 534:209–224

Matzeu A, Weiss F, Martin-Fardon R (2015) Transient inactivation of the posterior paraventricular nucleus of the thalamus blocks cocaine-seeking behavior. Neurosci Lett 608:34–39. doi:10.1016/j.neulet.2015.10.016

Matzeu A, Kerr TM, Weiss F, Martin-Fardon R (2016) Orexin-A/hypocretin-1 mediates Cocaine-seeking behavior in the posterior paraventricular nucleus of the thalamus via orexin/hypocretin receptor-2. J Pharmacol Exp Ther 359:273–279. doi:10.1124/jpet.116.235945

Moga MM, Weis RP, Moore RY (1995) Efferent projections of the paraventricular thalamic nucleus in the rat. J Comp Neurol 359:221–238

Neumann PA et al (2016) Cocaine-induced synaptic alterations in thalamus to nucleus accumbens projection. Neuropsychopharmacology 41:2399–2410. doi:10.1038/npp.2016.52

Nicola SM (2007) The nucleus accumbens as part of a basal ganglia action selection circuit. Psychopharmacology 191:521–550

Otake K, Nakamura Y (1998) Single midline thalamic neurons projecting to both the ventral striatum and the prefrontal cortex in the rat. Neuroscience 86:635–649

Padilla-Coreano N, Do-Monte FH, Quirk GJ (2012) A time-dependent role of midline thalamic nuclei in the retrieval of fear memory. Neuropharmacology 62:457–463. doi:10.1016/j.neuropharm.2011.08.037

Pape HC, Pare D (2010) Plastic synaptic networks of the amygdala for the acquisition, expression, and extinction of conditioned fear. Physiol Rev 90:419–463. doi:10.1152/physrev.00037.2009

Parent A, Sato F, Wu Y, Gauthier J, Levesque M, Parent M (2000) Organization of the basal ganglia: the importance of axonal collateralization. Trends Neurosci 23:S20–S27

Paxinos G, Watson C (2009) The rat brain in stereotaxic coordinates, 6th edn. Elsevier Academic Press, San Diego

Pecina S, Smith KS, Berridge KC (2006) Hedonic hot spots in the brain. Neuroscientist 12:500–511

Pennartz CM, Groenewegen HJ, Lopes da Silva FH (1994) The nucleus accumbens as a complex of functionally distinct neuronal ensembles: an integration of behavioural, electrophysiological and anatomical data. Prog Neurobiol 42:719–761

Penzo MA et al (2015) The paraventricular thalamus controls a central amygdala fear circuit. Nature 519:455–459. doi:10.1038/nature13978

Prensa L, Gimenez-Amaya JM, Parent A, Bernacer J, Cebrian C (2009) The nigrostriatal pathway: axonal collateralization and compartmental specificity. J Neural Transm Suppl:49–58

Reed MD et al (2015) Assessing contributions of nucleus accumbens shell subregions to reward-seeking behavior. Drug Alcohol Depend 153:369–373. doi:10.1016/j.drugalcdep.2015.05.001

Reichard RA et al (2016) Abundant collateralization of temporal lobe projections to the accumbens, bed nucleus of stria terminalis, central amygdala and lateral septum. Brain Struct Funct. doi:10.1007/s00429-016-1321-y

Reynolds SM, Berridge KC (2008) Emotional environments retune the valence of appetitive versus fearful functions in nucleus accumbens. Nat Neurosci 11:423–425

Shinonaga Y, Takada M, Mizuno N (1994) Topographic organization of collateral projections from the basolateral amygdaloid nucleus

to both the prefrontal cortex and nucleus accumbens in the rat. Neuroscience 58:389–397

Smith Y, Raju DV, Pare JF, Sidibe M (2004) The thalamostriatal system: a highly specific network of the basal ganglia circuitry. Trends Neurosci 27:520–527

Stratford TR, Wirtshafter D (2013) Injections of muscimol into the paraventricular thalamic nucleus, but not mediodorsal thalamic nuclei, induce feeding in rats. Brain Res 1490:128–133. doi:10.1016/j.brainres.2012.10.043

Su HS, Bentivoglio M (1990) Thalamic midline cell populations projecting to the nucleus accumbens, amygdala, and hippocampus in the rat. J Comp Neurol 297:582–593

Unzai T, Kuramoto E, Kaneko T, Fujiyama F (2017) Quantitative analyses of the projection of individual neurons from the midline thalamic nuclei to the striosome and matrix compartments of the rat striatum. Cereb Cortex 27:1164–1181. doi:10.1093/cercor/bhv295

Van der Werf YD, Witter MP, Groenewegen HJ (2002) The intralaminar and midline nuclei of the thalamus. Anatomical and functional evidence for participation in processes of arousal and awareness. Brain Res Brain Res Rev 39:107–140

Vertes RP, Hoover WB (2008) Projections of the paraventricular and paratenial nuclei of the dorsal midline thalamus in the rat. J Comp Neurol 508:212–237

Young CD, Deutch AY (1998) The effects of thalamic paraventricular nucleus lesions on cocaine-induced locomotor activity and sensitization. Pharmacol Biochem Behav 60:753–758

Zhu Y, Wienecke CF, Nachtrab G, Chen X (2016) A thalamic input to the nucleus accumbens mediates opiate dependence. Nature 530:219–222. doi:10.1038/nature16954